Investigating Spectroscopic and Structural Properties of Cr doped TiO_2 NPs Synthesized through Sol gel Deposition Technique

[1]Leta Tesfaye, [2]Bulcha Bekele, [3]Abel Saka, [4*]Krishnaraj Ramaswamy, [5]N. Nagaprasad, [6]K. Sivaramasundaram

[1, 2, 3] Department of Physics, Dambi Dollo University, College Natural and Computation Science, Ethiopia
[4] Department of Mechanical Engineering, Dambi Dollo University, College of Engineering Science, Ethiopia*
[5]Department of Mechanical Engineering, ULTRA College of Engineering and Technology, Madurai, 625104, Tamilnadu, India
[6]Department of Physics, ULTRA College of Engineering and Technology, Madurai, 625104, Tamilnadu, India

*Corresponding Author Email Id: r.kraj009@gmail.com

Abstract

This paper reports as prepared and Cr doped TiO_2 NPs at different doping concentrations of 0.02, 0.04, 0.06 and 0.08 mol% using simple technique called sol-gel method. The structural properties of as prepared and doped TiO_2 NPs were characterized through X-Ray Diffraction (XRD). The XRD results reveal that pure crystalline (anatase phase) was found in average crystal size range 12-14 nm which is calculated by Debye Scherrer formula. The lattice spacing of samples were decreased as Cr-doping concentration is increased corresponding to anatase phase (101) of the nanoparticles. The average crystal sizes of Cr-doped TiO2NPs were decreases with increasing doping concentrations. Spherical and uniformly distributed TiO_2 NPs were observed from SEM results which are good agreements with that of XRD results. The absorption spectra of as prepared and Cr doped TiO_2 NPs were investigated by UV/visible Spectroscopic photometer which enhance visible range of the absorption shifts to the red color as the doping concentrations increases. Additionally, energy band gap (Eg) of as prepared and doped nanoparticles were obtained from UV/visible which is decreased with increasing Cr dopant concentrations is due to decreasing particles size. Finally, defect states of prepared and doped TiO_2 NPs were Photo luminescence spectra.

Keywords: *Anatase phase, TiO_2 NPs, X-ray diffraction, UV/Visible*

1. Introduction

Titanium dioxide Nanoparticles (TiO_2NPs) are well known multi-functional nanoparticles because of its non-toxicity, ubiquity, and stability [1]. TiO_2 NPs have attractive application in photo catalysis, pigments, antireflection coatings, optical filters, and sensors applications. It has also large band-gap, chemically inert, photo-stable, inexpensive and high refractive index [2, 3]. In addition, TiO_2 NPs have been needed for polymer and dye-sensitized solar cells, hetero-junctions and hybrid organic-inorganic based solar cells, photo-catalysis application [4]. In nanotechnology, solar cells are one of the important of researchable areas due to its low-cost, simple to synthesis, have excellent efficiency of photo-conversion, have excellent properties like structural and electronic [2-4]. The three main structure of TiO_2 are rutile, anatase and brookite. Among these, anatase and rutile are commercially important due to its high energy band gap of 3.23 eV and 3.00 eV respectively [3-5]. It is also promising semiconducting material because of mainly its photo-stability and optical properties [6]. Not only TiO_2, but also ZnO, Ncb_2O_5 etc have excellent performance in solar cell activities of some semiconducting materials. Many researches were conducted by doping metal ion into TiO_2 with its modification on dye sensitive solar cell (DSSC) [7]. Here, there are acceptor dopants that produce photo-anode of dye sensitive solar cells. In other words, when iron, chromium, vanadium copper, zinc etc are doped with TiO_2, they are highly fabricating solar cells. Reduced TiO_2 NPs in to nano scale gives large surface to volume which is applicable in optical properties [1-5].

TiO_2 NPs absorbs UV-Radiation to its wide band-gap and the doping effects reduce the band gap energy. Furthermore, doping TiO_2 NPs by metals shows life-time electron and hole. In other words, the doping metal with TiO2 NPs ignores recombination of photo-excited charge carriers. Doping Cr in TiO NPs is important to obtain small bang gap by making shifting up of valence band and down conduction band and it makes easy to intrinsic properties in the visible region [1-6, 8]. Red-shifts of absorption band from UV to visible region is caused to charge transfer I conduction band to electron of doped TiO_2 [9]. Frankly speaking, several metal-ions are doped with TiO_2 NPs [6-9]. So, chromium has enhanced photo response in the range of visible wavelength leads narrow optical band-gaps. Several synthesizing technique are reported in several literatures. TiO_2 NPs can be synthesized by wet-chemical precipitation techniques, Chemical bath deposition techniques, Vapor pressure, mechano-chemical technique, hydrothermal techniques, Sol-gel technique etc. From these techniques, sol-gel deposition technique is the simplest methods, low costs and easy methods for the preparations on doped TiO_2NPs which gives photocatalytic and optical properties [10, 11]. From metallic ions, Cr gives high photo current density in visible region by optical absorption shifts. Moreover, there is an occurrence of valence electrons and valence band of TiO_2 were the excess holes creates an acceptor due to narrowing the band gapes between valence band and conduction bands [7, 9, 11].

Several papers present the impacts of temperature calcinations and Cr-doping for photo-catalyst results shifting towards high wavelength (red shift absorption edge) as the doping concentration was increased [12]. Like sol-gel method, chromium doped

titania was prepared for dye sensitive solar cells through hydrothermal technique results an increments in rutile phases while Cr-dopant were increased with improvements in electron life time and transportation mechanisms [13]. Similarly, Cr-doped Tio_2 nanoparticles were by sol-gel technique at dopant concentration (0.1, 0.5, 1.0 & 5.0 mol %) for absorption light results the formation of pure anatase phases (Raman spectroscopy & XRD results) and color centers were emerged from the UV/visible spectroscopic analysis [15]. As presented by Wu T et al. as prepared and Cr doped TiO_2 NPs were synthesized through hydrothermal approach for the purpose of structural and optical properties. The result shows the doped titanium dioxide Nanoparticles have excellent photocatalytic properties [16]. In addition Shuai C et al. reports room temperature synthesized TiO_2 NPs by Cr-doping through sol-gel technique were increases shifting of absorption band (red shift) to visible region as chromium doping increases. Uniformly anatase phase crystals of dope TiO NPs were observed from scanning electron microscopic result [17]. This experimental work presents, as prepared and Cr-doped TiO_2 NPs at doping concentration of 0.02, 0.04, 0.06 and 0.08 mol% through sol-gel deposition technique. The experimental details and Characterization techniques were investigated.

2. Experimental details

First titanium dioxide nanoparticles were prepared from acetic acid (CH_3COOH), titanium isopropoxide ($Ti[OCH(CH_3)_2]_4$) as Ti precursor and Chromium nitrate ($Cr(NO_3)_3.9H_2O$) as Cr precursor and used from preparations without further purifications. After this, for synthesis TiO_2 NPs (as prepared), 8 ml titanium isopropoxide were mixed with 16 ml of acetic acid. Then, solution was added to 16 ml of ethanol without touching the wall of the container and stirred by gentile magnetic stirrer for 2 hr. Then, the solution was settled at room temperature and gel-like substance was formed. The gel-like samples were washed three times by ethanol and it is now obligated to dry into oven at calcinations temperature of 160 ^oC for 6hr. Finally, the samples were brought to muffle Furnace (Model No: MC2-5/5/10-12, Biobase, Chaina) for 8 hr at calcinations temperatures of 400 ^oC. For preparing Cr doped titanium nanoparticles, chromium nitrate solution were prepared and mixed to TiO_2 solutions and stirred for 30 min. By similar procedure, Cr doped titanium dioxide nanoparticles were synthesized at different Cr concentration of 0.02, 0.04, 0.06 and 0.08 mol%. The synthesized samples were finally characterized by XRD (Model: D8 Advance Bruker, AXS, Germany), UV/Visible Spectroscopy (Model: Jasco, V 670, Japan), SEM (Model: Tecnai, G-2200 twin FEL, Netherlands) and photoluminescence.

3. Results and Discussion

3.1 X-Ray Diffraction Analysis

Figure 1 show XRD results of as prepared and Cr doped titanium dioxide nanoparticles at 0.02, 0.04, 0.06 and 0.08 mol% of chromium concentrations in the range of 20^o -80^o. As shown in figure (a, b, c, d, & e) the XRD result exhabits sharp diffraction peaks at diffraction angles of 18.86°, 31.58°,37.11°,44.91°, 59.54° and

65.20° with their corresponding reflection of (101), (103), (200), (105), (204) and (116) lattice plane which indicates the crystallinity of as prepared and doped nanoparticles respectively. These results manly investigate crystal size and crystal phase of as prepared and doped nanoparticles. The diffraction peaks reflects the formation of pure anatase phase and matched with (JCDS File No.900-9086, 500-0223 & 900-8123). Pure anatase phases are observed in all lattices planes which indexed in all diffraction patterns i.e. octahedral (Ti^{-6}) and trigonal planar (O^{-3}) geometry of host TiO_2. The crystal phase of pure TiO_2 NPs was unchanged in doping Cr in TiO_2 lattice. As the Cr doping concentrations increases, variation in intensity of diffraction peaks were formed with small shifts. This shifts cause slight expansion in unit cell volume due to the reduction of crystal size. In addition, unit cell volume expansion is quite doable to host titanium ions and ionic radii of chromium dopants [20].

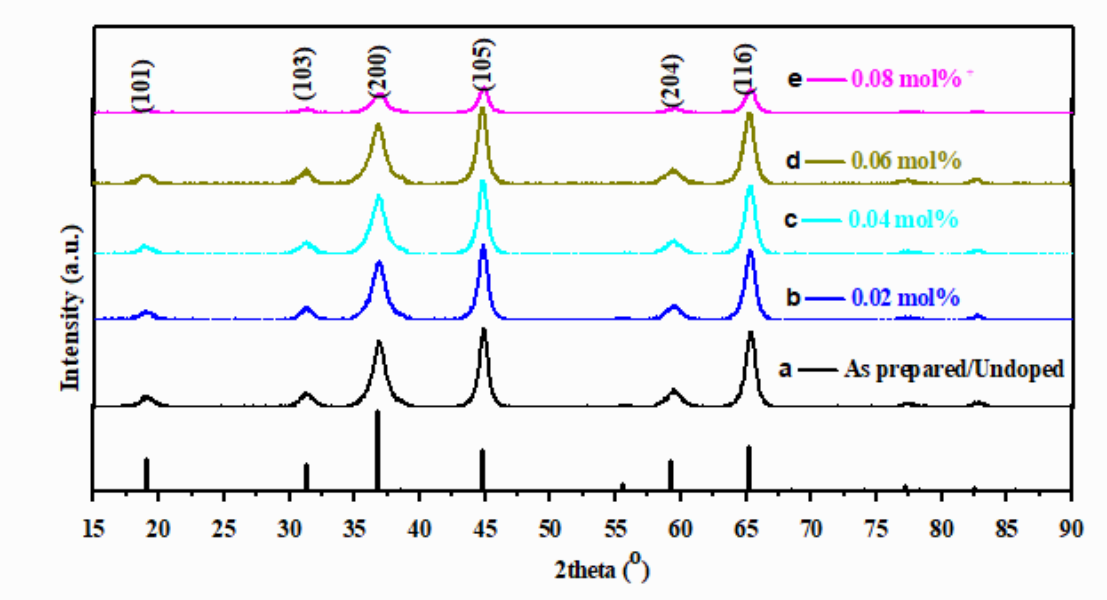

Figure.1. X-ray diffraction Patterns of as prepared and Cr doped TiO_2 NPs with dopant concentration of a. 0.02%, b. 0.04%, c. 0.06% and e. 0.08% mol.

The calculated ionic radii of Ti^{4+} and Cr^{3+} 60.8 and 59.7 pm are relatively close to each other. By substitution doping, Cr^{3+} enters lattices sites of Ti^{4+} [21]. Decreased intensity peaks with increasing full width at half maxima (FWHM) were observed from Cr-doped TiO_2 NPs is due to small sizes of the particles at which all Cr dopants does not enter the position of octahedral. Some Cr dopents are left on the grain boundaries or surfaces. Due the reduction of crystallite size, the crystal grows and their periodicities are distributed. Moreover, there is crystal impurities are observed. The crystallite size of as-prepared and Cr doped TiO_2 were calculated by using Debye Scherrer equation,

$$d = \frac{K\lambda}{\beta Cos\,\theta} \qquad (1)$$

Where the parameters $\boldsymbol{d}$, λ, β and θ are average crystallite size, wavelength X-ray wave length (0.15425 nm for Cu-Kα), full-width at half-maximum (FWHM) of the diffraction peak and the diffraction angle respectively. The calculated crystal sizes of as prepared and Cr-doped TiO_2 are 13.12, 12.86, 12.73, 12.70 and 12.50 nm related to the x-ray diffraction patterns of (a, b, c, d & e) as shown in figure 1 above respectively. The average crystal sizes of as prepared and Cr doped TiO_2 NPs are decreased as Cr doped concentrations are increased is good agreement to that of SEM results [22]. Wide diffraction peaks with small intensity were observed from XRD results as Cr doping increases are caused as a result of charge in ionic radius of Ti^{+4} and Cr^{+3}. Here, Cr doping concentration creates excess oxygen vacancies and neutralizes charge in TiO_2. [23]. Occupation of Cr^{+3} to titanium dioxide lattice results the absence of impurity peaks in diffraction patterns. At the saturate and moderate level, the photo-catalytic properties of doped nanoparticles increase as concentration increases. Finally, the lattice spacing distance d_{hkl} of as prepared and doped nanoparticles of anatase phase of results 0.379, 0.353, 0.347, 0.338 nm and 0.329 which decreases with increasing dopants.

3.2 Scanning Electron Microscopic Analysis

Figure 2 shows scanning electron microscopic analysis of as prepared and Cr-doped TiO_2 NPs at doping concentration of 0.02%.0.04%, 0.06% and 0.08% mol and the morphology of the particles are increases as the Cr-doping increases. From theoretical investigations, Cr doping on TiO_2 can be done through interstitial doping, substitution doping and isolated substitutional mechanisms. Theoretically, Compensating oxygen vacancy is observed during substitutional doping [24]. Therefore, Cr doped ions of TiO_2 nanoparticles can be understood from scanning electron microscope (SEM). The morphology, crystallinity and particles sizes of synthesized nanoparticles are investigated from SEM results. Therefore, SEM images reflects the formation uniformly distribution spherical shapes of nanoparticles with small agglomerations in the last two samples and it is reported that agglomerations observed in TiO2 NPs than the bulk titania. The particle sizes of as prepared and Cr doped titanium doped nanoparticles are less than 15 nm is the same as the XRD results.

3.3 UV/Vis Absorption Spectra Analysis

Figure 3 shows UV/Visible absorption spectra of as prepares and chromium doped titanium dioxide nanoparticles at the room temperature. The optical properties of the synthesized nanoparticles were determined from energy bang gap formula and the tendency of absorpting the UV radiation were mostly observed from as prepared sample as it has 3.2 eV band gap energy. The formation cut off UV/Vis wavelength of absorption spectra shows excitation of electrons.

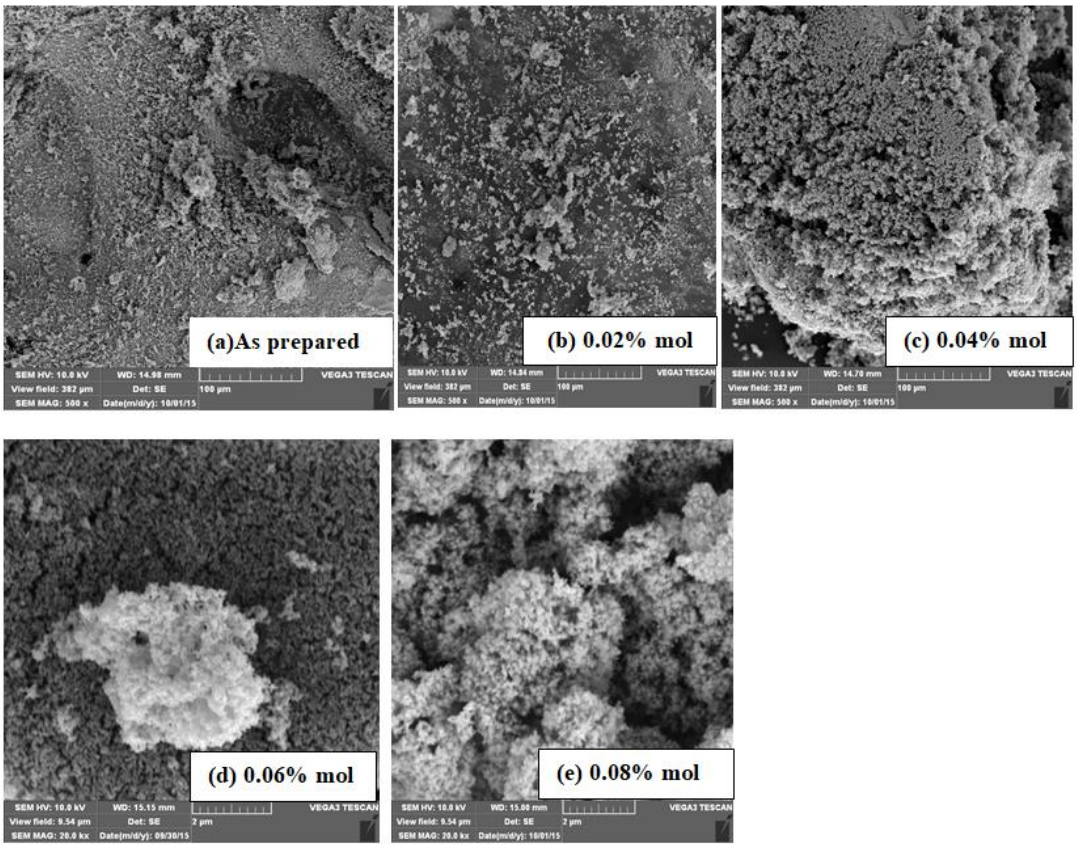

Figure.2. SEM images of as prepared and Cr doped TiO_2 at doping concentrations of 0.02%mol, 0.04%mol, 0.06%mol and 0.08 mol%

The photo-excitation of electron from conduction band to valence band. Furthermore, the electron excitation is formed by 3d→ 2g orbital of the Ti^{4+} cations in the conduction band while 2p orbital of the oxide anions are formed in valence band [25, 26]. Doped titanium nanoparticles reflect shifting towards high wavelength called red shift is due to chromium acceptance tendency of TiO_2. The amplitude of red shift absorption edge was increased with increasing doping concentrations. A red shift in absorption edge is due to conduction band of doped nanoparticles slightly gives reduced energy band gaps [27].

Table 1 show the optical band gap of as prepared and Cr-doped titanium dioxide nanoparticles using optical band gap equation.

$$E_g = h\frac{C}{\lambda} \qquad \textbf{(2)}$$

where E_g, h, c, and λ are band gap energy, blanks constant, speed of light, and wavelength spectrum of the absorption spectra respectively.

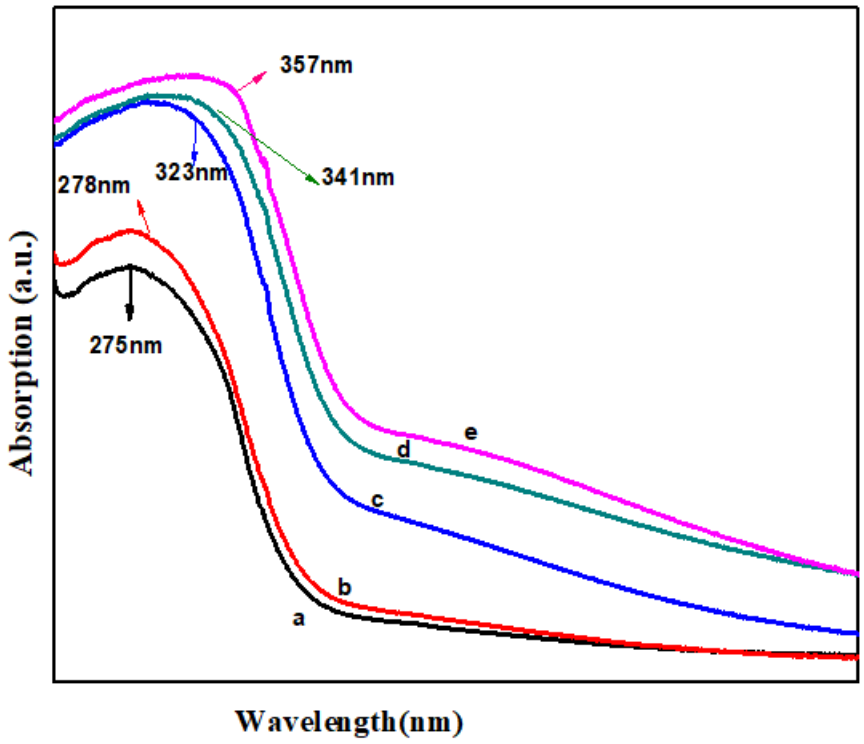

Figure 3. UV/visible absorbance spectra of a) as prepared and Cr-doped TiO_2 nanoparticles at dopant concentrations of b) 0.02 mol %, c) 0.04 mol%, d) 0.06mol%, and e) 0.08mol%.

Table 1. Wavelength, band gap energy of as prepared and chromium doped titanium dioxide nanoparticles

Sl.No.	Concentrations (%mol)	E_g (eV)
1	As prepared	3.30
2	0.02	3.29
3	0.04	3.26
4	0.06	3.21
5	0.08	2.94

As shown in table 1 above, the band gap energy of as prepared and chromium doped a Titanium dioxide is decreased as doping concentration increases and easily tuned to specific levels. As a result of optical absorption shifts, transitional metal ions like Cr doping concentration are observed in Ultraviolet to visible regions (28).

3.4 UV/Visible Transmittance Spectral Analysis

Figure 4 shows UV/Visible transmittance spectral analysis of as prepared and chromium doped titanium dioxide nanoparticles. The transmittance spectra of as prepared and doped nanoparticles are observed in Ultraviolet and visible region with having high transparency. Moreover, the transparency synthesized sample decreased with increasing Cr-dopant concentrations [29]. From the amplitude of transmition edge were decreased with increasing doping concentrations.

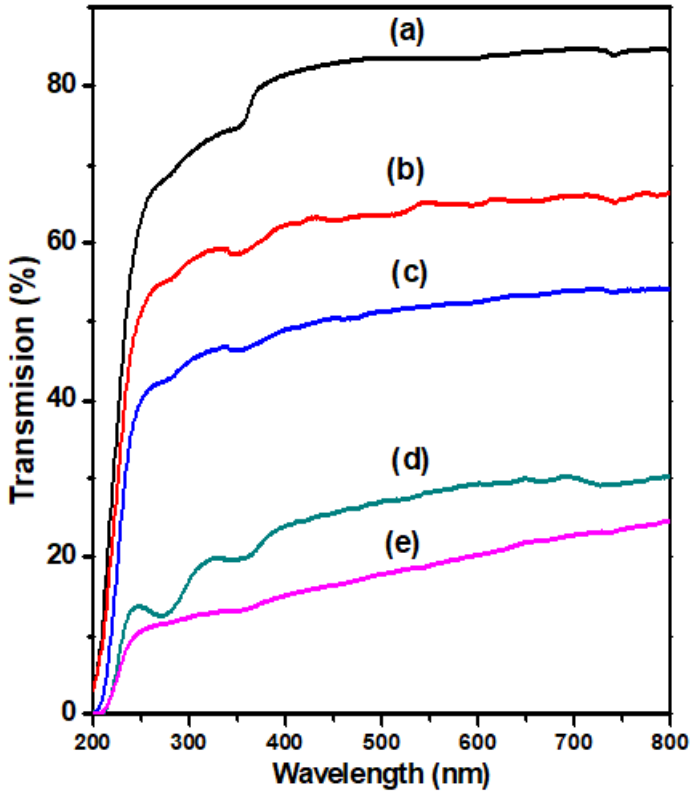

Figure 4. UV/Visible Transmittance spectra of as prepared and Cr doped TiO_2 NPs at doping concentrations of b) 0.02 mol%, c) 0.04 mol%, d) 0.06 mol%, and e) 0.08 mol%.

3.5 Photoluminescence Spectral Analysis

Figure 5 shows photoluminescence (PL) spectra of as prepared and chromium doping concentration of synthesized nanoparticles. PL emission spectra have been extensively used to show the charge transfer or electron-holes in semiconductor particles [30-32]. Again, PL shows as prepared and Cr-doped TiO_2 NPs and the curve pattern of Cr-TiO_2 similar to that of undoped anatase titanium dioxide nanoparticles. However, the PL intensity decreased significantly with increasing chromium doping. The intensity in 0.08mol% of Cr doped TiO_2 NPs was small which is most likely due to Cr atoms playing the role of electrons capturers where by depressing the

recombination process. Conversely, the intensity of undoped TiO_2 NPs was very large compared to the others [33-43].

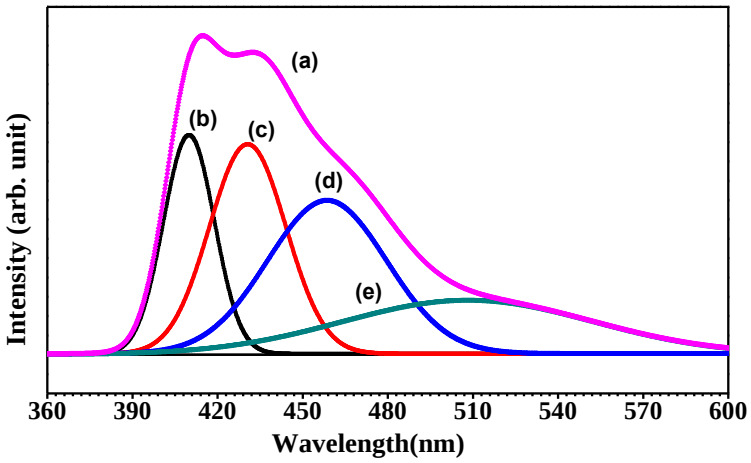

Figure 5. PL spectral analysis of a) as prepared and Cr doped TiO_2 NPs at dopant concentrations of b) 0.02 mol%, c) 0.04 mol%, d) 0.06 mol% and e) 0.08 mol%.

4. Conclusions

The sol gel deposition technique were followed to as prepare (undoped) and chromium doped titanium dioxide nanoparticles for investigating structural and spectroscopic properties. The synthesized samples were characterized by XRD, SEM, UV/Vis and PL. From XRD results, nanosized particles (11 -13 nm) and pure anatase crystal phase are synthesized at the same calcinations temperature. The particles sizes are obtained by using Scherrer's formula and decreases in particles size with increasing chromium dopant concentration. Wider diffraction peaks with small intensity were observed with an increament in chromium dopant and cause the change on ionic radii (Cr^{+3} & Ti^{+4}). The occupation of Cr^{+3} to the main TiO_2 lattice are due the presence purity or absence of purity of synthesized nanoparticles with and with-out doping chromium. Uniformly distributed/homogenous spherical shapes of as prepared and Cr-doped TiO_2 NPs were observed from SEM images. Around 0.379, 0.353, 0.347, 0.338 and 0.329 nm of lattice space were observed corresponding to as prepared and doped TiO_2 NPs of (111) of anatase phase. With increasing Cr-doping concentrations, the crystal size become decreased which is the same with that of XRD results. In addition, the bang gap energy of prepared samples were decreased as the chromium concentrations increases and shifted toward high wavelength or red shift. Finally, due to reduction band gap energy, transitional metal ions are easily tuned to TiO_2 lattice.

Acknowledgements

The authors would like to acknowledge staff of Dambi Dollo University for their indefinite support during our paper writing.

References

[1] *R. Yang, G. Jiang, J. Liu, Y. Wang, N. Jian, L. He and L. Liu L, "Plasmonic TiO_2@ Au NPs//CdS QDs photocurrent-direction switching system for ultrasensitive and selective photo-electrochemical bio-sensing with cathodic background signal", Analytica Chimica Acta. vol. 1153, **(2021)**, pp. 338283.*

[2] *M. Abidi, A. Hajjaji, A. Bouzaza, K. Trablesi, H. Makhlouf, S. Rtimi, A.A. Assadi and B. Bessais, "Simultaneous removal of bacteria and volatile organic compounds on Cu2O-NPs decorated TiO_2 nanotubes: Competition effect and kinetic studies", Journal of Photochemistry and Photobiology A: Chemistry. vol. 400, **(2021)**, pp.112722.*

[3] *Y.K Hashemi, M.T Yaraki, S. Ghanbari, L.H Saremi and M.H Givianrad, "Photodegradation of organic water pollutants under visible light using anatase F, N co-doped TiO2/SiO2 nanocomposite: Semi-pilot plant experiment and density functional theory calculations", Chemosphere. vol. 275, **(2021)**, pp.129903.*

[4] *K.N. Pandiyaraj, D. Vasu, R. Ghobeira, P.S.E. Tabaei, N. De Geyter, R. Morent, M. Pichumani, P.V.A. Padmanabhanan and R.R. Deshmukh, "Dye wastewater degradation by the synergetic effect of an atmospheric pressure plasma treatment and the photocatalytic activity of plasma-functionalized Cu–TiO2 nanoparticles", Journal of hazardous materials. vol. 405, **(2021)**, pp.124264.*

[5] *M. Nemiwal, T.C. Zhang and D. Kumar, "Recent Progress in g-C3N4, TiO2 and ZnO based Photocatalysts for Dye Degradation: Strategies to Improve Photocatalytic Activity", Science of the Total Environment. vol. 767, **(2021)**, pp. 144896.*

[6] *D. Xu, S. Yang, Y. Su, Y. Xiong and S. Zhang, "Catalytic conversion of plastic wastes using cost-effective bauxite residue as catalyst into H_2-rich syngas and magnetic nano-composites for chrome (VI) detoxification", Journal of hazardous materials. vol. 413, **(2021)**, pp.125289.*

[7] *E.T. Helmy, E.M Abouellef, U.A Soliman and J.H Pan, "Novel green synthesis of S-doped TiO2 nanoparticles using Malva parviflora plant extract and their photocatalytic: antimicrobial and antioxidant activities under sunlight illumination", Chemosphere. vol. 71, **(2021)**, pp.129524.*

[8] *L. Jiang, Z. Luo Z, Y. Li, W. Wang, J. Li, J. Li, Y. Ao, J. He, V.K. Sharma and J. Wang, "Morphology-and Phase-Controlled Synthesis of Visible-Light-Activated S-doped TiO2 with Tunable S4+/S6+ Ratio", Chemical Engineering Journal. vol. 402, **(2020)**, pp.125549.*

[9] *H. Shi, T. Zhao, J. Wang, Y. Wang, Z. Chen, B. Liu, H. Ji, W. Wang, G. Zhang and Y. Li, "Fabrication of g-C3N4/PW12/TiO2 composite with significantly enhanced photocatalytic performance under visible light", Journal of Alloys and Compounds. vol. 860, **(2021)**, pp.157924.*

[10] *G.J. Thangamani and S.K. Pasha, "Titanium Dioxide (TiO2) Nanoparticles Reinforced Polyvinyl Formal (PVF) Nano-composites as Chemiresistive Gas Sensor for Sulfur Dioxide (SO2) Monitoring", Chemosphere. vol. 275, **(2021)**, pp. 129960.*

[11] *I.P. Mahendra, A. Huda, H.M. Ngoc, P.T. Nghia, T. Tamrin and B. Wirjosentono, "Investigation of TiO_2 doped with nitrogen and vanadium using hydrothermal/Sol-Gel method and its application for dyes photo-degradation", Arab Journal of Basic and Applied Sciences. vol. 26, **(2019)**, pp. 242-253.*

[12] *T.D. Chu, D.T. Quach, X.T. Nguyen, T.S. Nguyen, D.T. Pham and D.H. Kim, "Synthesis and Properties of Magnetic-Semiconductor Fe_3O_4/TiO_2 Heterostructure Nano-composites for Applications in Wastewater Treatment", Journal of Magnetism and Magnetic Materials. vol. 25, **(2020)**, pp.1-7.*

[13] *A. Hashim, H. Abduljalil and H. Ahmed, "Fabrication and characterization of (PVA-TiO2) 1-x/SiCxnanocomposites for biomedical applications", Egyptian Journal of Chemistry. vol. 63, **(2020)**, pp. 71-83.*

[14] *J.A. Yuwono, P. Burr, C. Galvin and A. Lennon, "Atomistic Insights into Lithium Storage Mechanisms in Anatase, Rutile, and Amorphous TiO2 Electrodes", ACS Applied Materials & Interfaces. vol. 13, **(2021)**, pp.1791-1806.*

[15] *D.C. Nguyen, T.L.L. Doan, S. Prabhakaran, D.T. Tran, D.H. Kim, J.H. Lee and N.H. Kim, "Hierarchical Co and Nb dual-doped MoS_2 nano-sheets shelled micro-TiO2 hollow spheres as effective multifunctional electro-catalysts for HER, OER, and ORR", Nano energy. vol. 82, **(2021)**, pp.1057-50.*

[16] *T. Wu, H. Zhao, X. Zhu, Z. Xing, Q. Liu, T. Liu, S. Gao, S. Lu, G. Chen, A.M. Asiri and Y. Zhang, "Identifying the origin of Ti3+ activity toward enhanced electrocatalytic N2 reduction over TiO2 nanoparticles modulated by mixed-valent copper", Advanced Materials**.** vol. 32, **(2020)**, pp. 200-299.*

[17] *C. Shuai, B. Wang, S. Bin, S. Peng and C. Gao, "TiO2-Induced In situ reaction in graphene oxide-reinforced AZ61 bio-composites to enhance the interfacial bonding", ACS Applied Materials & Interfaces. vol. 12, **(2020)**, pp. 23464-23473.*

[18] *S. Hejazi, S. Mohajernia, B. Osuagwu, G. Zoppellaro, P. Andryskova, O. Tomanec, S. Kment, R. Zboril and P. Schmuki, "On the Controlled Loading of Single Platinum Atoms as a Co- Catalyst on TiO2 Anatase for Optimized Photocatalytic H2 Generation", Advanced Materials. vol. 32, **(2020)**, pp. 190-505.*

[19] *L. Cao, K. Xu and M. Fan, "ZnO.5Cd.5S nanoparticles modified TiO_2 nano-tube arrays with efficient charge separation and enhanced light harvesting for boosting visible-light-driven photo-electrochemical performance", Journal of power sources. vol. 482, **(2021)**, pp. 228956.*

[20] *K. Zhou, W.L. He, X. Zhang, B. Zhang, X.N. Gong, K.W. Wang, Z.C. Zhang, X.L. Zhang, Z.N. Xia and X.Y. Zhou, "Photocatalytic and photochemical processes of AgCl/TiO2 studied with a fully integrated X-ray photoelectron spectrometer", Rare Metals. vol. 3, **(2021)**, pp. 1-9.*

[21] *P.A. Vinosha, R. Ragu, S. Kalaiarasi, B. Xavier and S.J. Das, "Shock induced TiO_2 nanoparticles and its synergistic effect in photo-voltic application", Chemical physics letters. vol. 754,* ***(2020)****, pp. 137644.*

[22] *Y. Jiang, H. Pang, X. Sun, Z. Yang, Y. Ding, Z. Liu and P. Zhang, "TiO_2 nano-belts with ultra-thin mixed C/SiOx coating as high-performance photo/photo electro-chemical hydrogen evolution materials", Applications of surface science. vol. 537,* ***(2021)****, pp. 147861.*

[23] *W. He, K. Wang, Z. Zhu, H. Zou, K. Zhou, Z. Hu, Y. Duan, Y. Feng and L. Gan,. "Ultra-small subnanoTiO x clusters as excellent cocatalysts for the photocatalytic degradation of tetracycline on plasmonic Ag/AgCl", Catalysis Science & Technology. vol. 10,* ***(2020)****, pp. 147-153.*

[24] *Y. Dong and F. Meng, "Synthesis and photocatalytic properties of three dimensional laminated structure anatase TiO2/nano-FeO with exposed (001) facets", RSC advances. vol. 10,* ***(2020)****, pp.11823-11830.*

[25] *V.S. Raghuwanshi, U.M. Garusinghe, W. Batchelor and G. Garnier, "Polyamide-amine-epichlorohydrin (PAE) induced TiO_2 nanoparticles assembly in cellulose network", Journal of Colloid and Interface Science. vol. 575,* ***(2020)****, pp. 317-325.*

[26] *H.K. Sung, Y. Lee, W.H. Kim, S.J. Lee, S.J. Sung, D.H. Kim and Y.S. Han, "Enhanced Power Conversion Efficiency of Dye-Sensitized Solar Cells by Band Edge Shift of TiO2 Photoanode", Molecules. vol. 25,* ***(2020)****, pp. 1502.*

[27] *J.A. Godoy, A. Pereira, M. Gomes, M. Fraga, R. Pessoa, D. Leite and G. Petraconi, "Black TiO_2 Thin Films Production Using Hollow Cathode Hydrogen Plasma Treatment: Synthesis, Material Characteristics and Photocatalytic Activity", Catalysts. vol. 10,* ***(2020)****, pp. 282.*

[28] *M. Fan, Z. Lin, P. Zhang, X. Ma, K. Wu, M. Liu and X. Xiong, "Synergistic Effect of Nitrogen and Sulfur Dual-Doping Endows TiO2 with Exceptional Sodium Storage Performance", Advanced energy materials. vol. 11,* ***(2021)****, pp. 2003037.*

[29] *F. Lan, H. Zhang, J. Fan, Q. Xu, H. Li and Y. Min, "Electrospun Polymer Nanofibers with TiO2@NiCo-LDH as Efficient Polysulfide Barriers for Wide-Temperature-Range Li–S Batteries", ACS Applied Materials & Interfaces. vol. 13,* ***(2021)****, pp. 2734-2744.*

[30] *G.L. Di, G. Zaccariello, A. Benedetti, G. Vecchiotti, F. Caposano, E. Sabbioni, F. Groppi, S. Manenti and Q. Niu, "Genotoxicity and Immunotoxicity of Titanium Dioxide-Embedded Mesoporous Silica Nanoparticles (TiO2@ MSN) in Primary Peripheral Human Blood Mononuclear Cells (PBMC)", Nanomaterials. vol. 11,* ***(2021)****, pp. 270.*

[31] *M.E. El-Naggar, A.R. Wassel and K. Shoueir, "Visible-light driven photocatalytic effectiveness for solid-state synthesis of ZnO/natural clay/TiO2 nanoarchitectures towards complete decolorization of methylene blue from aqueous solution", Environmental nanotechnology monitoring & management. vol. 15,* ***(2021)****, pp. 100425.*

[32] *M. Tabish, G. Yasin, M. Bilal, T.H. Nguyen, C.P. Van, P. Nguyen-Tri, R.K. Gupta and T.A. Nguyen, "A facile strategy for the construction of TiO2/Ag nano-hybrid-*

*based polyethylene nanocomposite for antimicrobial applications", Nano-Structures & Nano-Objects. vol. 25, **(2021)**, pp.100671.*

[33] *J. Wang, X. Li, Y. Ren, Z. Xia, H. Wang, W. Jiang, C. Liu, S. Zhang, Z. Li, S. Wu and N. Wang, "The effects of additive on properties of Fe doped TiO2 nanoparticles by modified sol-gel method", Journal of Alloys and Compounds. vol. 858, **(2021)**, pp.157726.*

[34] *R. Venkatarama, R. Krishnaraj, M. sakthivel, K. Kanthavel R. Palani, "Enhanced ERP for paper Machines", International Journal of Scientific & Engineering Research. Vol. 2, **(2011)**, pp. 1-10.*

[35] *C.M. Balamurugan, R. Krishnaraj, M. Sakthivel, K. Kanthavel, R. Palani, "Computer aided modeling and optimization analysis", International Journal of Scientific & Engineering Research. Vol. 2, **(2011)**, pp. 1-8.*

[36] *M.M. Thilak ,R. Krishnaraj, M. Sakthivel, K. Kanthavel, R. Palani, "Transient thermal and structural analysis of the rotor Disc of Brake", International Journal of Scientific & Engineering Research. Vol. 2, **(2011)**, pp. 1-4.*

[37] *M.G. Deepan Marudachalam, K. Kanthavel, R. Krishnaraj, "Optimization of shaft design under fatigue loading using Goodman method", International Journal of Scientific & Engineering Research. Vol. 2, **(2011)**, pp. 1-5.*

[38] *P. Dharmalingam, K. Kanthavel, R. Sathiyamoorthy, M. Sakthivel, R. Krishnaraj, C. Elango, "Optimization Of Cellular Layout Under Dynamic Demand Environment By Simulated Annealing", International Journal of Scientific & Engineering Research. Vol. 3, **(2012)**, pp. 1-7.*

[39] *S. Varatharajan, R. Krishnaraj, M. Sakthivel, K. Kanthavel, M.G. Deepan Marudachalam,R. Palani, "Design and Analysis of single disc machine top and bottom cover", International Journal of Scientific & Engineering Research. Vol. 2, **(2011)**, pp. 1-6.*

[40] *LT. Jule, R. Krishnaraj, N. Nagaprasad, S. Vigneshwaran, V. Vignesh, "Design and analysis of serial drilled hole in composite material", Materials Today Proceeding.**(2021)**, https://doi.org/10.1016/j.matpr.2021.02.587.*

[41] *LT. Jule, R. Krishnaraj, Bulcha Bekele, Abel Saka, N. Nagaprasad, "Experimental Investigation on the Impacts of annealing temperatures on titanium dioxide nanoparticles structure, size and optical properties Synthesized through Sol-gel methods", Materials Today Proceeding. **(2021)**, https://doi.org/10.1016/j.matpr.2021.02.586.*

[42] *B. Stalin, N. Nagaprasad, V. Vignesh, M. Ravichandran, "Evaluation of mechanical and thermal properties of tamarind seed filler reinforced vinyl ester composites", Journal of Vinyl and Additive Technology. Vol. 25, **(2019)**, pp. E114-E128.*

[43] *N. Nagaprasad, B. Stalin, V. Vignesh, M. Ravichandran, N. Rajini, O. Ismail, "Effect of cellulosic filler loading on mechanical and thermal properties of date palm seed / vinyl ester composites", International Journal of Biological Macromolecules. Vol. 147, **(2020)**, pp. 53-66.*